Al-Nahrain Journal for Engineering Sciences **NJES** 27(1)1-8, 2024
http://doi.org/10.29194/NJES.27010008

Drop Size Distribution in Agitated Contactor: A Review

Marwa S. Hamed[1a*], Basim O. Hasan[1b], Hussein T. Znad[2], Sahir M. Al-Zuraiji[3]

Authors affiliations:
1) Chemical Engineering Department, Al-Nahrain University, Baghdad, Iraq.
a*)marwasalam199431@gmail.com
b) basimohasan13@gmail.com

2) WA School of Mines: Minerals, Energy and Chemical Engineering, Curtin University, Perth, WA, 6845, Australia.
H.Znad@curtin.edu.au

3) Surface Chemistry and Catalysis Department, Centre for Energy Research, Budapest, Hungary.

Paper History:

Received: 2nd April. 2023

Revised: 5th May. 2023

Accepted: 22nd May 2023

Abstract

The breakage rate of liquid drops in the dispersed phase is a key way to improve the heat and mass transfer between the continuous/dispersed phases. This work includes a review of experimental results of liquid drop breakage in an agitated tank. The study highlighted the experimental conditions that were investigated as well as the important findings about the impact of operating conditions on some breakup parameters. The conflicts and discrepancies in the findings of those studies were identified and analyzed. The review found that many experimental parameters affect the drop breakage rate. The breakage probability (BP), number of fragments, and breakage time (BT) are direct functions of power input.

Keywords: Stirrer Tank, d_{32}, Breakage Time, Breakage Probability

توزيع حجم القطرة في الموصل المهتاج: مراجعة

مروه سلام حمد*، باسم عبيد حسن، حسين توفيق زناد، ساهر محمد الزريجي

الخلاصة:

يعد معدل تكسر قطرات السائل في المرحلة المشتتة طريقة أساسية لتحسين انتقال الحرارة والكتلة بين المراحل المستمرة / المشتتة. يتضمن هذا العمل مراجعة النتائج التجريبية للكسر المتساقط للسائل في الخزان المتحرك. سلطت الدراسة الضوء على الظروف التجريبية التي تم التحقيق فيها وكذلك النتائج الهامة حول تأثير ظروف التشغيل على بعض معاملات الانهيار. تم تحديد وتحليل التعارضات والتناقضات في نتائج تلك الدراسات. وجدت المراجعة أن العديد من المعلمات التجريبية تؤثر على معدل الانكسار المتساقط. بالإضافة إلى ذلك ، فإن احتمال الكسر (BP) وعدد الشظايا ووقت الكسر (BT) هي وظائف مباشرة لإدخال الطاقة.

1. Introduction

It happens frequently in several industries, including chemical, food, petroleum, and pharmaceutical ones, for immiscible fluids to disperse in turbulent liquid flows. The sizes of the generated drops produced by drop breakage in turbulence affect transport phenomena [1]. The mother drop behaves differently when subjected to varying shear forces and turbulent fields, beginning with initial deformation and leading to the first breakup that produces two fragments (daughter bubbles). The breakage process can continue to yield the ultimate number of fragments from the final breaking event [2]. The strength of the shear force and the turbulent eddies that interact with the drops determine the number and size distribution as well as the local breaking behavior [3].

The primary causes of drop breakage have been hypothesized to be turbulent fluctuations and eddy-particle collision. High kinetic energy eddies have been used to describe turbulence. Eddy-particle interaction results from the interaction of the eddy with fluid particles. The momentum of the continuous phase changes, and the drop changes its shape. The drop surface becomes unstable when the value of the oscillations is high enough, at which point it stretches to form a neck and fragments into several daughter droplets [4]. The local differences in velocities cause the stresses that are applied to the particles. There are four possible outcomes when a particle interacts with turbulent eddies. The fluid particle can produce considerable deformation and breakage by interacting with several small turbulent eddies [5,3].

Over several decades, great modeling efforts have been directed toward studying and attempting to simulate the drop breakage phenomenon in various mixers. The vast majority of known experimental studies on drop breakup studies, characterized the breakage phenomena by determining the diameter of the generated bubble (d_{32} or d_{max}) and by the number of produced drops.

The breakage time is considered a crucial factor in determining the breakage rate. The time duration between the start of the mother particle's deformation and the breakage that produces the final population of fragments is referred to as the breakage time [6]. Experimentally calculating the breakage time is always a more effective technique to determine the breakage probability [7].

NJES is an **open access Journal** with **ISSN 2521-9154** and **eISSN 2521-9162**

2.The geometry of the stirred tank

The stirred tank show in Figure (1) is made up of a cylindrical flat bottom tank with its diameter (D_T). The second part is rectangular baffles (their width, $W_{BF}=D_T/10-D_T/12$), baffles are symmetrically spaced and inserted around the tank's perimeter to avoid vortex formation. The number of inserted baffles used can range from zero to four. The most important part that makes up the mixing tank is the impeller which has a diameter range of $D_T/4$- $D_T/2$ and an off-bottom clearance of a range of $D_T/6$-$D_T/2$. The clearance (C) is defined as the distance between the bottom of the tank and the centerline of the blades [8]. The rotating impeller transfers the mechanical energy into the bulk liquid and causes mixing by momentum transfer motion. Regardless of the impeller type used, the generated streams flow in three directions, namely, rotational flow, radial flow, and axial flow. For an unbaffled stirred tank the tangential velocities generated by turbine impellers are high relative to radial and axial components and the circumferential flow is dominated [8]. This type of flow leads to vortex formation and drains gas from the surrounding ambiance at high speeds. Symmetrical wall baffles are usually installed inside the tank to avoid vortex formation and fluid swirling [8,9]. The baffles reduce the tangential velocity and almost with no changes in the radial components to ensure even distribution and create turbulence during transitional and turbulent mixing [10,11].

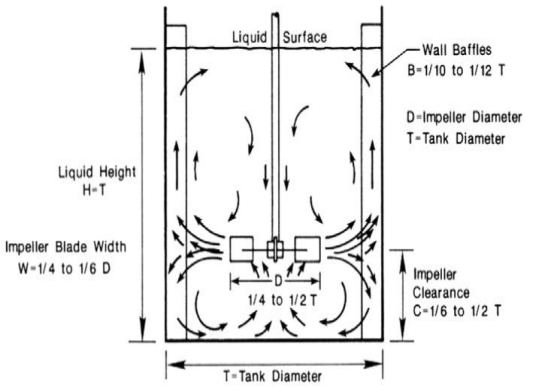

Figure(1): A diagram of the stirred vessel with a standard Rushton turbine [1].

3. Main findings of previous works

This work includes a review of drop breakup for the recent twenty years in stirred tank systems and discusses the effect of drop breakage by determining d_{32} and d_{max}, BP, generated fragments number, and breakup time. Earlier research on the fluid-particle breakup in stirred tanks is summarized in Table 1 in appendix. It consists of the conditions examined in each paper, the two-phase system, the size of the experimental apparatus, and the breakage characterization. parameters chosen, and the measurement method employed.

3.1. Sauter mean diameter (d_{32}) and maximum diameter (d_{max})

The Sauter mean diameter d32 is by definition the ratio of the third to the second moment of the probability density function the value of d_{32} is related to the factors affecting the size distribution of particles or droplets in a system**.**

d_{32} is extensively used in the characterization of liquid/liquid or gas/liquid dispersions. This usage arises because it links the area of the dispersed phase to its volume and hence to mass transfer and chemical reaction rates. the Sauter mean diameter depends both on d_{min}, d_{max}, and the shape of the drop size distribution. The complexity of dispersion processes in stirred vessels under turbulent conditions does not allow a theoretical description of the full drop size distribution[24]. It has been widely used to express the breakage rate through d_{32} and d_{max} in the turbulent field. Determining d_{32} and d_{max} depicts the phenomenon of breakage for getting a better understanding [25].

Previous studies revealed that drop breakage is a function of different operating parameters such as the physical properties of dispersed and continuous phases, the tank's geometry, the power input, and the time of exposure to the turbulence field. [12] found that the d_{max} is the same for both large and small impellers. Interfacial tension increases d_{max} linearly [13], show that the d_{max} for the pure breakup process decreases with time. For different size impellers, the small and large d_{max} values are related to the inverse of impeller speed.

[21] show the course of the mean diameter is dependent on the number of drops used for averaging as presented in Figure(2) . The minimum number of drops that is necessary to evaluate was determined for each impeller rotational speed for both impellers. [26] It was found that the type of liquid phase is the main factor that affects the bubble size distribution and, it found that the values of the Sauter mean diameter increased due to an increase in the superficial air velocity for air-water systems. finally, the value of d_{32} depends on the specific system and conditions. However, in general, increasing the surface tension or viscosity of the dispersed phase tends to result in larger particle or droplet sizes and a higher value of d_{32}, while increasing the surface tension or viscosity of the continuous phase tends to result in smaller particle or droplet sizes and a lower value of d_{32}. The method of particle or droplet generation and the design of the equipment can also have a significant impact on the size distribution and value of d_{32} [27].

[15] reported that the daughter drop diameter increased with dispersed phase percentage and decreased with agitation time. [6] show for mother a drop of size 0.6-4 mm. Uneven-sized breakups were more common than equal-sized ones. Multiple breakups were more common than binary ones. [22] indicated that as the mother droplet size increased, the daughter droplets became larger.

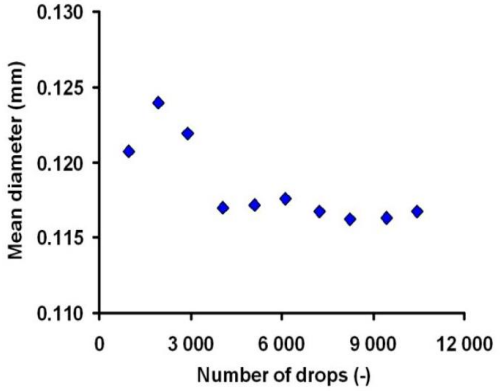

Figure (2): Determination of a minimum number of drops – principle (Rushton turbine, N = 150 rpm)[21].

3.2. The breakup probability (BP)

Counting the number of broken bubbles provides a simple method for calculating the breakage probability from experimental observation. The BP is the number of breakages occurring to the total number of injected single mother drops. To calculate breakage probability, only the first breakage is considered. Previous works found that the BP varied with the operating conditions. There is a consensus among the academic result that the probability of breakage increases in proportion to an increase in either the power input or the turbulence level. High-velocity oscillations in the high-turbulence area increase the chance of eddy-drop contact. When the blade tip is close, the high effect causes breakage; when it's far, turbulent eddies of velocity fluctuation do. It's hard to distinguish between the two, making particle breakup difficult to identify. The mother fluid particle advances slowly toward the blade tip before breaking apart there, usually from blade collision or sheer force. High stirring speeds push the mother particle away from the wall, where impeller tip flow currents break it apart. At high stirring speeds, the mother surface velocity differential is still functional. Even at low stirring speeds, anisotropic turbulence in the stirred tank causes mother drops to break up far from the impeller. drops can be propelled close to the blade edge by flow currents and eddies, where they can fragment into many pieces.

High-speed imaging holds promise for assessing fluid particle fracture in agitated pipes. This technique helped researchers find the fracture process, especially amid strong turbulence. High-speed cameras can detect fluid particle movement even at high agitation speeds. Imaging technology has benefits and cons. [14] studied breakage probability and breakage time for the three systems (Toluene/water, Paraffin oil 10/ water, and Paraffin oil 100/ water) at dp = 1.0 mm, u_{fluid} = 1.5 m/s. It was found to be 60, 58, and 26, respectively. The breakage probability in decreases with increasing droplet stability. [22] determined the probability of producing different numbers of fragments versus operating parameters. It implies that in the other systems studied in this study, the binary breakup was dominant. This is because the findings of multiple breakages being dominant were based primarily on single-drop breakup experiments in which the diameter of the droplets was much larger than the drop swarm under steady-state. [28] reported that the BP is dependent on impeller geometry, blade number, and Re. Different bubble breakup rates are produced by different blade geometries. Variations in impeller power inputs and flow hydrodynamics at high Re, a four-flat blade impeller has an 86% BP. In the work of [3], high BP was observed in front of the blade's tip, with approximately 90% of breakages occurring within 0.35Ri of the blade's tip (where Ri is the impeller radius). [29] The breakage probability (BP) of the 4 mm mother bubble at 340 rpm was found to be increased by 12.61 percent. [30] found that at the impeller region, the BP in both oil and water is 100%. In general, the probability of multiple breakages in the oil phase is slightly lower than in water. The investigation of the Weber number value on the BP revealed that high-viscosity paraffin oil 100 has by far the lowest breakage probability [31]. Weber's numbers range from 0.6 to 2.2. Probabilities are compared by[32]. [33] found that at the smallest Weber number, the BP gradually increased until it reached 1 for a Weber number close to 50. Breakup probabilities were found to increase with to We-number up to 50% at We= 4 [23]. [31] for a low Weber number, the probability of breakage is high. The authors had similar results for low Weber number values, with the lowest data point exhibiting no breakages at Weber number values ranging from 0.8 to 3.2. The breakage probability was 9% for Weber number values 3.2-6.4, increasing to 60% for Weber number values 16-24.

3.3. The breakage time (BT)

The literature describes many methods for calculating the breakage time, and as a result, on many occasions, it contrasts the experimentally determined values. [34] defined BT to start from the beginning of the extra deformation that causes the drop breakup to the moment of the first breakage. [7] considered the BT from the moment the drop entered the impeller region until the breakage occurrence. [6] defined the duration of time that elapses between the initial stage of a spherical drop's deformation and its final breakup as the breakage time. [35] revealed that increasing the mother drop size causes an increase in the residence time in the turbulent field leading to an increase in the BP. The breakage time values were affected in various ways by the shape and the agitation velocity. [7] reported that the breakage time decreases nonlinearly with increasing drop size. [6] observed that when the mother drop size rises, the breakage time increases. When the mother size increased to a significant level, there was a minimum in the trend that indicated a significant rise in breakage time. In addition, petroleum drop had a longer breakup time than toluene due to its higher viscosity and surface tension. [36] found that because of the mother bubble's

trajectory is affected by the breakup time rises, the breakage zone is also affected. [14] studied breakage time for the three investigated systems (Toluene/water, Paraffin oil 10/ water, and Paraffin oil 100/ water) at dp = 1.0 mm, u_{fluid} = 1.5 m/s). The authors found the breakage time to be 3.4, 3.8, and 8.5 ms, respectively. In addition, the breakage time is significantly increased for the high-viscosity paraffin oil. That could be one explanation for the outstanding breakage location distributions of the high-viscosity paraffin oil 100/water system.

When deformation starts in the region of high turbulence level, a breakup occurs away blade. Breakage initiation correlates with the maximum local energy dissipation rates. [6] regarded the breaking time from the last breakage event as the comparatively substantial deformation that caused the breakage. [37] reported that the breakage time decreases when impeller Re and had no systematic trend with the size of the mother bubble. The BT ranged between (42 and 74 ms) for the investigated mother bubble size and Re. The time between the first and last breakage is dependent on both Re and mother bubble. [29] observed breakage BT decreased by 60% as the impeller velocity increased, reaching 19.8 ms at 340 rpm. [15] show a single 2-mm toluene drop is introduced into the breakage cell at a constant velocity of the continuous phase of 1.5 m/s. After it passes the section of the disc turbine, the drop breaks into several daughters drop via a breakup cascade. Figure (3) shows this behavior. Figure (4) shows the breakage time of an image sequence of a breakage event. First, an initially spherical drop is deformed and breaks into two near-equal daughters. In this instance, the breakage is ended according to the initial breakage event definition. One of the daughters continues with a deformation process and an additional smaller drop is produced.

In this instance, the event is considered to end in the cascade breakage event definition, as no more breakages occur. [23]

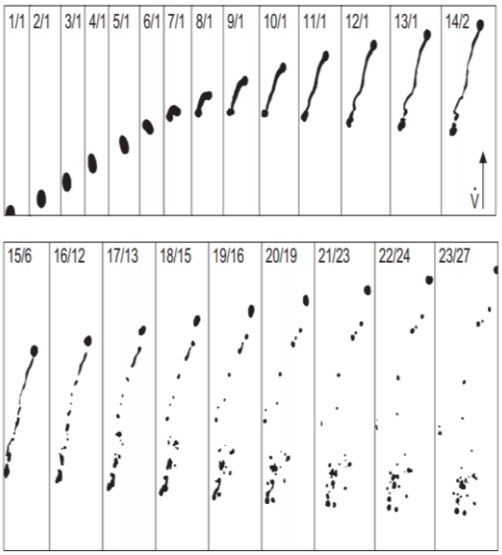

Figure (3): A breakage cascade is used to divide the drop into multiple daughters drops[15].

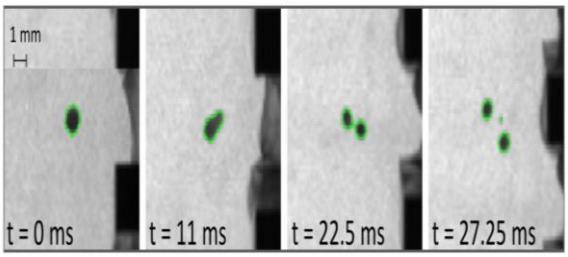

Figure (4): Breakage time a 0.99 mm in diameter mother drop. [23]

3.4 Number of fragments

Power input and mother drop size both affect how many fragments (daughter drops) are produced due to the breakage. The number of fragments grows over time as the mother drop experiences repeated breakages. The quantity of daughter bubbles grows as Re increases. This is likely caused by the faster rate of energy dissipation, which encourages fragmentation. [38] found that the average daughter drop size increased as the mother drop size increased.

More fragments are created when the mother drop's size is greater [39]. According to the authors, breaking a mother's drop into many daughters' drops requires more energy. A drop must enter a zone with considerable energy dissipation to break. The smaller the mother drop, the lower the number of daughter drops, the lower the drop size, and the lower BP. Only binary bubble breakups occurred in [34] turbulent pipe flow systems. [22] it has been reported that viscosity can have a significant impact on the number of fragments during the breakup of a single large drop. There appears to be agreement that viscous droplets tend to stretch into a thread, resulting in a large number of droplets. [40] drop breakdown was investigated in a stirred-loop reactor tank. The number of daughter drops increased as the mother drop size (13 mm), viscosity, and impeller speed increased. [41] investigated the breakup for low values of Weber numbers. The mean number of generated fragments increased as the Weber number increased. [33] investigated drop breakup in pipe flow and found that the average number of daughter drops was 12. [7] investigated single-drop breakage in a swirled liquid-liquid tank. 60% of the 0.56 mm mother drops disintegrated into two daughter drops. A 2 mm mother drop gave birth to 97 daughter drops. In turbulent tank conditions, the authors discovered a link between the number of daughter drops and the size of the mother drops: the probability of binary breakdown increased with smaller mother drops. Multiple splits outnumbered binary splits. The most daughter drops were more than nine. Bubbles in a stirred tank were investigated [6]. [5] Static mixer breakups and drop breakups were investigated. The experiment found that the majority of bubble breakups resulted in a binary. Multiple breakups were more likely than binary breakups for drops (average of 3.2 fragments). For 2.5-3.4 mm mother bubble diameters, multi-breakage increases with tank energy dissipation rate (0.5, 0.9,

and 1.4 m^2 s^3). Reported that the particles continue to fragment until the hydro-mechanical stresses are unable to overcome the coherence forces that hold the particle drop. [16] reported that a maximum of 12 daughter bubbles were formed as a result of the breakup [6]. [29] found that at 340 rpm, a mother bubble of 4 mm produced 22 fragments. [30] found that in the case of the oil continuous phase, the average number of fragments at a speed of 430 rpm is 9.2, while in the case of water, it is 12.4.

4. Conclusions

From the current review, investigators have recently worked hard to understand and define how drops break up in agitated tank systems. Despite years of intensive research, many aspects of the phenomenon are still poorly understood. The visualization studies using high-speed imaging have led to a successful determination of breakup parameters. However, they still contradict the results obtained due to the complexity of the drop breakup phenomena. The review showed that the number of breakages increases with the increase in the size of the mother drop and the speed of agitation (or Re). The most important conclusion reached through this review is that the d_{max} is the same for both large and small impellers. Unequal-sized breakups were more common than equal-sized breakups. Multiple breakups were more common than binary when the mother droplet size increases. There is a consensus among the experimental results that the breakup probability increases in proportion to the rise in either the power input or the turbulence level. The breakup probability (BP) on impeller geometry, blade number, and Re, and the studies all agree that increasing the Re increases the BP. When the mother size rises, the breakage time (BT) decreases. Most previous works showed that BT decreases with increasing Re and has no systematic trend with the size of the mother bubble. The quantity of daughter bubbles grows as Re increases. The smaller the mother drop, the lower the number of daughter drops, the lower size, and the lower probability of breakage. There appears to be an agreement that viscous droplets tend to stretch into a thread, resulting in a large number of droplets. More scientific efforts using are still required to better understand the drop breakup mechanism and the effect of operating conditions.

References

[1] J. Solsvik and H. A. Jakobsen, "Single drop breakup experiments in stirred liquid-liquid tank," *Chem. Eng. Sci.*, vol. 131, pp. 219–234, 2015.
[2] A. Rivière, W. Mostert, S. Perrard, and L. Deike, "Sub-Hinze scale bubble production in turbulent bubble break-up," *J. Fluid Mech.*, vol. 917, 2021.
[3] B. O. Hasan, M. F. Hamad, H. S. Majdi, and M. M. Hathal, "Experimental characterization of dynamic behavior of single bubble breakage in an agitated tank," *Eur. J. Mech.*, vol. 85, pp. 430–443, 2021.
[4] H. Zhou, X. Yu, B. Wang, S. Jing, W. Lan, and S. Li, "Experimental study on drop breakup time and breakup rate with drop swarms in a stirred tank," *AIChE J.*, vol. 67, no. 1, 2021.
[5] R. Andersson and B. Andersson, "Modeling the breakup of fluid particles in turbulent flows," *AIChE J.*, vol. 52, no. 6, pp. 2031–2038, 2006.
[6] J. Solsvik, P. J. Becker, N. Sheibat-Othman, I. Mohallick, R. Farzad, and H. A. Jakobsen, "Viscous Drop Breakage in Liquid–Liquid Stirred Dispersions: Population Balance Modeling," *J. Dispers. Sci. Technol.*, vol. 36, no. 4, pp. 577–594, 2015.
[7] S. Maaß and M. Kraume, "Determination of breakage rates using single drop experiments," *Chem. Eng. Sci.*, vol. 70, pp. 146–164, 2012.
[8] P. M. Doran, *Bioprocess engineering principles*. Elsevier, 1995.
[9] D. Zhao, B. Azzopardi, Y. Yan, H. Morvan, R. F. Mudde, and S. Lo, *Hydrodynamics of gas-liquid reactors: normal operation and upset conditions*. John Wiley & Sons, 2011.
[10] E. L. Paul, V. A. Atiemo-Obeng, and S. M. Kresta, *Handbook of industrial mixing: science and practice*, vol. 1. John Wiley & Sons, 2003.
[11] L. Li and B. Xu, "Numerical analysis of hydrodynamics characteristics in a top-covered unbaffled stirred tank," *Chem. Pap.*, vol. 75, no. 11, pp. 5873–5884, 2021.
[12] P. Patil and S. Kumar, "Breakup of drops around the edges of Rushton turbine," *Can. J. Chem. Eng.*, vol. 88, no. 6, pp. 912–918, 2010.
[13] P. D. Patil and S. Kumar, "Continued self-similar breakup of drops in viscous continuous phase in agitated vessels," *Chem. Eng. Sci.*, vol. 66, no. 20, pp. 4932–4935, 2011.
[14] S. Hermann, S. Maaß, D. Zedel, A. Walle, M. Schäfer, and M. Kraume, "Experimental and numerical investigations of drop breakage mechanism," in *1st International Symposium on Multiscale Multiphase Process Engineering (MMPE), Kanazawa, Japan*, 2011, pp. 4–7.
[15] S. Maaß, N. Paul, and M. Kraume, "Influence of the dispersed phase fraction on experimental and predicted drop size distributions in breakage dominated stirred systems," *Chem. Eng. Sci.*, vol. 76, pp. 140–153, 2012.
[16] A. Daub, M. Böhm, S. Delueg, and J. Büchs, "Measurement of maximum stable drop size in aerated dilute liquid–liquid dispersions in stirred tanks," *Chem. Eng. Sci.*, vol. 104, pp. 147–155, 2013.
[17] A. Bąk and W. Podgórska, "Drop breakage and coalescence in the toluene/water dispersions with dissolved surface active polymers PVA 88% and 98%," *Chem. Eng. Res. Des.*, vol. 91, no. 11, pp. 2142–2155, 2013.
[18] A. Daub, M. Böhm, S. Delueg, M. Mühlmann, G. Schneider, and J. Büchs, "Maximum stable drop size measurements indicate turbulence attenuation by aeration in a 3 m3 aerated stirred tank," *Biochem. Eng. J.*, vol. 86, pp. 24–32, 2014.
[19] H. Tokanai and M. Kuriyama, "Sizes of maximum stable drops with different flow behavior in liquid–liquid agitation," *J. Chem. Eng. Japan*, vol. 48, no. 4, pp. 257–261, 2015.

[20] J. Solsvik, S. Maaß, and H. A. Jakobsen, "Definition of the single drop breakup event," *Ind. Eng. Chem. Res.*, vol. 55, no. 10, pp. 2872–2882, 2016.
[21] E. Bucciarelli, R. Formánek, B. Kysela, I. Fořt, and R. Šulc, "Dispersion kinetics in a mechanically agitated vessel," *EPJ Web Conf.*, vol. 213, p. 02008, 2019.
[22] H. Zhou, J. Yang, S. Jing, W. Lan, Q. Zheng, and S. Li, "Influence of Dispersed-Phase Viscosity on Droplet Breakup in a Continuous Pump-Mixer," *Ind. Eng. Chem. Res.*, vol. 58, no. 51, pp. 23458–23467, 2019.
[23] E. H. Herø, N. La Forgia, J. Solsvik, and H. A. Jakobsen, "Single oil drop breakage in water: Impact of turbulence level in channel flow," *Chem. Eng. Sci. X*, vol. 12, p. 100111, 2021.
[24] A. W. Pacek, C. C. Man, and A. W. Nienow, "On the Sauter mean diameter and size distributions in turbulent liquid/liquid dispersions in a stirred vessel," *Chem. Eng. Sci.*, vol. 53, no. 11, pp. 2005–2011, 1998.
[25] M. Martín, F. J. Montes, and M. A. Galán, "Influence of impeller type on the bubble breakup process in stirred tanks," *Ind. Eng. Chem. Res.*, vol. 47, no. 16, pp. 6251–6263, 2008.
[26] T. J. Mohammed, F. Z. Hanna, and I. B. Hamawand, "Bubble Size Distribution in Gas-Liquid Dispersion Column," *J. Eng.*, vol. 18, no. 7, 2012.
[27] S. Hall, A. W. Pacek, A. J. Kowalski, M. Cooke, and D. Rothman, "The effect of scale and interfacial tension on liquid–liquid dispersion in in-line Silverson rotor–stator mixers," *Chem. Eng. Res. Des.*, vol. 91, no. 11, pp. 2156–2168, 2013.
[28] H. A. Alabdly, H. S. Majdi, M. F. Hamad, M. M. Hathal, and B. O. Hasan, "Effect of impeller geometry on bubble breakage and the contributions of different breakage mechanisms in a stirred tank," *Fluid Dyn. Res.*, vol. 52, no. 6, p. 65504, 2020.
[29] A. M. Mhawesh, B. O. Hasan, and H. Znad, "Hydrodynamics of Stirred Tank and Bubble Breakup Behavior Induced by Rushton Turbine," *Al-Nahrain J. Eng. Sci.*, vol. 25, no. 1, pp. 35–43, 2022.
[30] B. O. Hasan, "Single Bubble Breakage in Oil Under Stirring Conditions," *Al-Nahrain J. Eng. Sci.*, vol. 25, no. 1, pp. 6–11, 2022.
[31] M. Ashar, D. Arlov, F. Carlsson, F. Innings, and R. Andersson, "Single droplet breakup in a rotor-stator mixer," *Chem. Eng. Sci.*, vol. 181, pp. 186–198, 2018.
[32] S. Galinat *et al.*, "Breakup of a drop in aliquid–liquid pipe flow through an orifice," *AIChE J.*, vol. 53, no. 1, pp. 56–68, 2007.
[33] S. Galinat, O. Masbernat, P. Guiraud, C. Dalmazzone, and C. Noı, "Drop break-up in turbulent pipe flow downstream of a restriction," *Chem. Eng. Sci.*, vol. 60, no. 23, pp. 6511–6528, 2005.
[34] R. P. Hesketh, A. W. Etchells, and T. W. F. Russell, "Experimental Observations of Bubble Breakage in Turbulent Flow," *Ind. Eng. Chem. Res.*, vol. 30, no. 5, pp. 835–841, 1991.
[35] M. Konno, M. Aoki, and S. Saito, "Scale effect on breakup process in liquid-liquid agitated tanks," *J. Chem. Eng. Japan*, vol. 16, no. 4, pp. 312–319, 1983.
[36] J. F. Walter and H. W. Blanch, "Bubble break-up ingas—liquid bioreactors: break-up in turbulent flows," *Chem. Eng. J.*, vol. 32, no. 1, pp. B7–B17, 1986.
[37] B. O. Hasan, "Experimental study on the bubble breakage in a stirred tank. Part 1. Mechanism and effect of operating parameters," *Int. J. Multiph. Flow*, vol. 97, pp. 94–108, 2017.
[38] V. Hančil and V. Rod, "Break-up of a drop in a stirred tank," *Chem. Eng. Process. Process Intensif.*, vol. 23, no. 3, pp. 189–193, 1988.
[39] B. O. Hasan, "Breakage of drops and bubbles in a stirred tank: A review of experimental studies," *Chinese J. Chem. Eng.*, vol. 25, no. 6, pp. 698–711, 2017.
[40] M. Kuriyama, M. Ono, H. Tokanai, and H. Konno, "The number of daughter drops formed per breakup of a highly viscous mother-drop in turbulent flow," *J. Chem. Eng. Japan*, vol. 28, no. 4, pp. 477–479, 1995.
[41] A. Zaccone, A. Gäbler, S. Maaß, D. Marchisio, and M. Kraume, "Drop breakage in liquid-liquid stirred dispersions: Modelling of single drop breakage," *Chem. Eng. Sci.*, vol. 62, no. 22, pp. 6297–6307, 2007.

Appendix

Table (1): Experimental studies of drop breakage in stirred tank system

Authors	Experimental equipment	Operating conditions	The two phases	Breakage characterization parameters	The measuring technique (s)
[12]	4 baffle, D_T = 105 mm and 127 mm, 6 blade impellers, D_i =(40,50,70)mm (Rushton), H = D_T.	N = (100 –700) rpm , addition 0.3% SDS, μ_d = (1.07–156) mPa·s, σ = (2.7–7.1) mN/m T = room temperature, Φ = 3%	Continuous phase: 60% sugar syrup Dispersed phase: sunflower oil	dmax	sampling technique
[13]	4 baffle, D_T = 105 mm and 127 mm, 6 blade impellers, D_i = 40 mm, 50 mm, 70 mm (Rushton), H = D_T.	N = (0.7–1.5) m/s, addition 0.3% SDS, agitation time = (1–30) h., Φ = 3%	Continuous phase: 60% sugar syrup. Dispersed phase: sunflower oil	dmax	sampling technique
[14]	Tank of flat bottom, 4 baffles, H = D_T D_T = 150 mm, 6 blades	N = (400–770) rpm , dp = (0.5–3.1) mm ,T = 20 °C, Φ = 20%,	Continuous phase: distilled water Dispersed phase: toluene	d_{32}	sampling technique

	impeller, D_i = 50 mm, C = 50 mm,				
[15]	Curved bottom tank, 4 baffles, D_T = 155 mm, 6 blades impeller, D_i = 93 mm	PVA = 300 mg/kg, t = (1–1170) min, N = (250–410) rpm, addition of surfactant(PVA), T = 20 °C, Φtol. = (0.05–0.45), Φ of others = (0.05 – 0.2)	Continuous phase: water Dispersed phase: anisole, cyclohexane, n-butyl chloride, and toluene)	d_{32}	High-speed camera
[16]	dished bottom, 4 baffles, D_T = 293 mm, filling volume = 0.35 m^3 , 3 Rushton turbine impellers, D_i = 104 mm, C = 95 mm	$\mu_{par.}$ = 0.107 Pa·s, agitation rate = 4.2 to 10 s_{-1} Q_g = 0.7 vvm pH = 7.3, T = 25 °C	Continuous phase: water containing 1 mmol·L^{-1} PO_4 Dispersed phase: paraffin oil	dmax	sampling technique
[17]	D_T = 150 mm = H, 6 Rushton blade impellers, 4 baffled,	t = (1–180) min, PVA concentration = 0.001% –0.1%, N = (350 –700)rpm, hydrolysis = 88% and 98%, T = 25 °C,	Continuous phase: water Dispersed phase: toluene	d_{32}	High-speed camera
[18]	dished bottom D_T = 1.2 m, 4 baffles, filling volume (2.4–2.8) m^3, 3 impeller types of 6 blades in one shaft, D_i = (0.41, 0.51) m. Clearance: C_1 = 0.51, C_2 = 1.2, C_3 = 1.89	$\mu_{par.}$ = 0.107 Pa·s /m^3 , t =3h ,Q_g = (0.1–1) vvm, power input =(0.3 – 6.3) Kw/m^3 , pH = 7.3, T = 25 °C, Φ = (0.001–0.003) m^3	Continuous phase: water containing 1 mmol·L−1 PO_4 Dispersed phase: paraffin oil	d_{max}	sampling technique
[6]	The tank of flat bottom, 4 baffles BW= is 11mm 6 impeller blades C= 4 cm Di= 50 mm D_T=143 mm	ε (m^2/s^3) =1.14 T= 298 K ϱ (kg/m^3) = Toluene 866.7 Petroleum 754 n-Dodecane 745 1-Octanol 822 σ = (mN/m) Toluene 33 Petroleum 44.5 n-Dodecane 41.5 1-Octanol 8.4 μ = (mPa s) DKH, Toluene 0.60 Petroleum 1.14 n-Dodecane 1.38 1-Octanol 7.52 N= 650 rpm	Continuous phase: distilled water Dispersed phase: petroleum, toluene, n-dodecane, and 1-octanol.	Probability (%) of binary and multiple breakups And the Breakage time	a high-speed camera
[19]	The horizontal vessel, 4 baffles, Rushton turbine, 4 blade propellers, D_i = 63.5 mm, D_T = 127 mm H = 127 mm	N = (300–900) rpm, T = 20 °C, μ_c = (2.23–3.13) mPa s, t = (17–500) min.	Continuous phase: turpentine oil Dispersed phase: plastic liquids.	d_{32} and d_{max}	high-speed camera
[20]	Stirred Tank, Baffles, Rushton turbine Diameter of mother drop toluene/water (0.65, 1.0, 2.0, 3.0) petroleum/water (0.54, 0.7, 1.0, 1.3, 1.9, 3.1)	U=1.5 m/s σ [mN/m] = toluene 32 petroleum 38.5 n-dodecane 41.5 μ[mPa·s] = toluene 0.55 petroleum 0.65 n-dodecane 1.38	Continuous phase: water Two oils were used in the dispersed phase: toluene (99.98% purity) and petroleum (99.9% purity)	number of daughters drops and breakup time	high-speed camera

	C= 1 m	ϱ[kg/m^3] = toluene 870 petroleum 790 n-dodecane 745 ε =0.9 - 1.4 m^2 s^{-3}. N= (600, 650, and 700 rpm)	Both oils were blended with a non-water-soluble black dye		
[21]	baffled cylindrical flat bottom, vessel, T = 300 mm, 4 baffles, H = T. Di = 100 mm, C /D = 0.85. B/T was 0.1.	For Water ρ=998(kg/m^3), μ=0.955 *10^{-3} (Pa.s),σ=7.2 * 10^{-2} (N/m), For Silicone oil,WACKER AP 200, ρ= 1 070 (kg/m^3) μ= 0.214 x 10^{-3} (Pa.s) ,σ= 3.5 x 10^{-2} (N/m), Φ = 0.047 %	Continuous phase: water Dispersed phase: silicone oil	d_{32} and dmax	image analysis
[22]	a square tank .Di= 65mm 8 blades with 10 mm high and 2 mm thickness Mixer tank 100× 100× 100 mm Buffer chamber 100× 100× 30 mm Image region 5.5× 14.7× 10 mm	ϱ_d (kg/m^3)= (٩٠٢,٩٣٩,,٩٤٨,٩٦٢ ٩٦٢,٩٦٣,٧٨٢,٨٠٦ ٨٢٦,840,٨٥١) respectively μ (mPa·s) = (3.67,10.0, 26.7,86.0,86.0,315 3.25,7.04,13.46 30.55,58.34) respectively σ(mN/m) = (30.21,36.57,36.42 31.28,31.28,32.14 31.89,44.65,45.79,46.19 51.61) respectively N (rpm)= (390,420,600) T=25 °C and at atmospheric pressure The total feed flow rate 500 mL/min	Continuous phase: The deionized water Dispersed phase: silicone oil_1 silicone oil_2 silicone oil_3 silicone oil_4 silicone oil_5 30vol% paraffin oil / n-dodecane 75vol% paraffin oil / n-dodecane 90vol% paraffin oil / n-dodecane paraffin oil	Probability, d_{32}	A high-speed camera
[23]	The channel is 1 m long with a cross-section of 30 mm by 30 mm and the rods are 3 mm by 3 mm spaced evenly every 10 mm.	Properties of 1-octanol dyed with Sudan Black Density, ϱ = 825 kg/m^3 ,μ= 9.09 10^{-3} kg/ (m s) σ = 8.20 mN/m. U [m/s] = 1,1.5,2 the continuous phase ϱ= 1000 kg/m^3 Mother Drop Size[mm]=(1,1.48,1.78,2.23 0.87,1.13,0.86,1.02)	Continuous phase: reverse osmosis tap water Dispersed phase: 1-octanol	the breakage probability, the average number of fragments, the size distribution,	high-speed camera